

# Twin Grid-array as 3.6 GHz Epidermal Antenna for Potential Backscattering 5G Communication

Jack D. Hughes<sup>†</sup>, Cecilia Occhiuzzi\*, John Batchelor<sup>†</sup>, Gaetano Marrocco\*

**Abstract**—Emerging 5G infrastructures can boost innovative paradigms for future wearable and epidermal devices exploiting low-power (even passive) wireless backscattering-based communication. To compensate high body- and path-losses, and to extend the read range, array configurations are required. This work proposes a flexible monolithic epidermal layout, based on Krauss array concept, that operates at 3.6 GHz and it is suitable to be directly attached to the human body. The antenna involves a dual grid configuration with a main radiating grid backed by a grid reflector placed in touch with the skin. Overall, the amount of conductor and dielectric substrate are minimized with benefit to breathability. The antenna is suitable to surface feeding and produces a broadside radiation. Parametric analysis are performed and an optimal configuration of four-cells grid is derived and experimentally demonstrated to provide a maximum gain of more than 6 dBi.

**Index Terms**—Epidermal electronics, flexible electronics, epidermal array antenna, 5G antenna.

## I. INTRODUCTION

Epidermal Electronics [1] is an emerging research trend aimed at developing medical devices in a soft, flexible and sometimes stretchable format for direct on-skin application. These devices are often passive, referring to a system without a battery, working on harvested power alone, hence reducing impact on energy, waste, and pollution whilst requiring minimal maintenance [2]. The mostly used communication strategy in this regard is backscattering coding, which allows an epidermal node to transmit data by reflecting and modulating an incident RF wave [3]. Nowadays, backscattering communication is widely deployed in the UHF band (860-960MHz) by Radio-Frequency Identification (RFID) Technology and can be considered a reference platform for epidermal devices [4] thanks to the absence of batteries, the minimal electronics, the sensing capabilities, and the possibility to reach a read distance of up to 1-2 m. Coupling this with currently developing fifth generation (5G) communication systems makes body-centric communication an unprecedented opportunity for both leisure and medical applications [5]. It is expected that future 5G devices will be able to interact with epidermal devices via battery-less backscattering communications, granting the capability to retrieve multiple bio-physical electrical signals or track muscles and body motions in real-time and with high-accuracy [6]. Preliminary studies have demonstrated

that the new 5G frequency within the S-band (3.6 GHz) has advantages over UHF RFID [6] for backscattering links involving epidermal tags. Namely, in spite of the higher free space attenuation, 3.6 GHz antennas are suitable to provide comparable read distance to on-skin UHF, whilst boasting smaller layout and much higher data-rate.

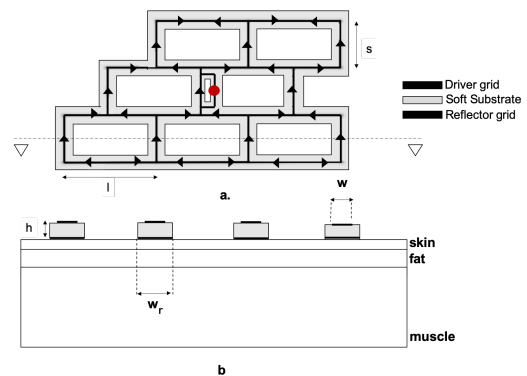


Figure 1. Schematic representation of the twin-grid antenna array and pattern of currents. Feed is planar and located on the central element through a T-match impedance transformer. a) Top view; b) Section with the three layers numerical body phantom adopted in FDTD simulations (CST Microwave Studio)

One – lambda loops are largely recognized as suitable for epidermal antennas [7]. Studies in the UHF and 5G S bands demonstrated that optimal loop configurations exist [8], [6]. Namely, at 3.6 GHz a maximum radiation gain of  $G_{max} \approx -5dB$  can be achieved with a single miniaturized  $17.5 \times 17.5 \text{ mm}^2$  loop placed 0.25 mm from the body. To improve gain, mitigate path and body losses, and obtain greater communication distances, multiple antennas in array configuration can be adopted. Preliminary numerical results in [6] investigated the upper bound performances achievable by varying the number of array elements, however no attempt has been made to engineer and prototype a final layout with the required beam forming network.

Typical array configurations for body-centric communications include patches and slot antennas [9]. At higher frequencies, more directive layouts such as Yagi-Uda or 3D layouts have been also proposed [10]. However, their structures lack the required flexibility to conform to the body; furthermore they integrate large conducting ground planes (or EBG structures [11]) making it difficult for the skin to breathe, also requiring complicated and intricate feed networks for proper functionality. Even if mitigation can be obtained by exploiting textile materials and flexible substrates [12], their application

\*University of Roma “Tor Vergata”, DICII, Via del Politecnico 1, Rome  
e-mail: [cecilia.occhiuzzi@uniroma2.it](mailto:cecilia.occhiuzzi@uniroma2.it)

<sup>†</sup> University of Kent, EDA, Jennison Building, Canterbury, Kent, CT2 7NT  
e-mail: [jdh23@kent.ac.uk](mailto:jdh23@kent.ac.uk)

This work was supported by the University of Rome Tor Vergata within “Beyond Borders-Epidermal Sensor Networks for Emerging 5G systems,” under Grant E84I19002410005.

to epidermal electronics is still in question.

Recently, the authors [13] proposed the use of a *monolithic* epidermal array (layout in Figure 1) that is based on loop antennas arranged as a Kraus grid [14]. Kraus grid has found application at mm-wave frequency for antenna-in package technology [15] thanks to high gain, bandwidth, simple feed, low profile, lightness and relatively straightforward construction. However, the presence of the ground plane introduces a challenge for epidermal applications as it makes the device more rigid and less breathable. A ground-less configuration for on-skin applications was hence numerically investigated at 60 GHz [13], since the skin is highly reflective at this frequency it operates as the ground-plane. At 3.6 GHz, the electromagnetic interaction with the body cannot be neglected and the removal of the ground plane would greatly reduce the radiation efficiency. To overcome this limitation, this paper proposes and experimentally evaluates a new array layout with a twin-structure comprising of a *driver* (radiating) grid and a *reflector* grid. The reflector grid still partially decouples the antenna from the body maintaining the broadside radiation of the Kraus grid, with the benefit of leaving most of the area uncovered by conductors and substrate. To make the device compatible with surface-mounted electronics, the antenna is fed at the middle of the central vertical element through a coplanar impedance transformer.

The paper is organized as follows. In Section II the layout of the epidermal grid array is presented, together with a parametric analysis devoted to defining the upper bound performances. A synthesis of a microstrip-grid array antenna is then presented in Section III. The paper concludes with prototypes and measurements in realistic conditions.

## II. ANTENNA LAYOUT

The proposed twin-grid array has a continuous structure consisting of *loop cells* with dimensions  $s \approx \lambda_{wg}/2$  and  $l = 2s$ ,  $\lambda_{wg}$  is the guided wavelength [16] at the centre frequency of operation  $f_0$ , evaluated under the simplified hypothesis of a continuous (full) ground under the grid and by considering the microstrip width  $w$  and the thickness  $h$  of the substrate [15], staggered by  $\lambda_{wg}/2$  between rows as to make the shape shown in Figure 1. The structure is resonant, the currents on vertical elements are in phase and act as radiators, while couplets of horizontal currents are in phase reversal acting as transmission lines. To partially decouple the antenna from the human body, a twin-grid is adopted as a reflector in direct contact with the human skin. Between the grids a lightweight, flexible and biocompatible substrate is included (silicone rubber, with permittivity  $\epsilon_r = 3$  and  $\tan \delta = 1.4 \cdot 10^{-3}$ ). Both substrate and reflector follow the driver shape, leaving uncovered a large part of the skin surface benefiting the breathability and wearability of the antenna and enabling the possibility to directly access the human body through sensors. Finally, the grid is fed from the antenna centre through a T-match impedance transformer [17] for fine tuning and control of the input impedance.

The radiation performance of the twin-grid array has been preliminary evaluated with the aim to find the optimal size

of both driver and reflector. Numerical simulations include a  $150 \times 150 \times t_h \text{ mm}^3$  3-layers body phantom [6] (Skin  $t_h = 1\text{mm}$ ,  $\epsilon_r = 36.92$ ,  $\tan \delta = 2.08$  - Fat  $t_h = 3\text{mm}$ ,  $\epsilon_r = 5.16$ ,  $\tan \delta = 0.16$  - Muscle  $t_h = 31\text{mm}$ ,  $\epsilon_r = 51.32$ ,  $\tan \delta = 2.65$  shown in Figure 1(b). Analysis is carried out by varying the number of loop-cells  $N$  and the width of the reflector conductor  $w_r$ . With attention focused on the radiation only, the grid is considered in transmitting mode and simply fed on the central vertical element without an impedance transformer, to be inserted later on.

### A. Optimal number of cells

The starting point is a resonant 1-cell layout with parameters  $\{h = 2\text{mm}, s = 28.45\text{mm}, l = 56.9\text{mm}, w = 1\text{mm}, w_r = 8\text{mm}\}$ , placed on a  $h = 2\text{mm}$  thick ( $\sim \lambda_{wg}/25$ ,  $\lambda_{wg} \approx 56\text{mm}$ ) bio-silicone rubber slab. The gain increases with the number of elements  $N$  (Figure 2): moving from 1 cell (a single loop – with two vertical radiators) to eight cells (15 radiators) an improvement of about 8 dB is obtained. Similar to standard grids with continuous ground [18], the  $G(N)$  profile is not linear since the increase of gain is limited by the attenuation of currents on the microstrip lines and by the poor control over the phase synchronization in case of large array. Furthermore, coherently with what was experienced with epidermal single layouts [6], the radiation performances of a skin array is the result of the balance between the array effect itself and power loss into the human body. The initial increase in the efficiency and gain is mostly due to the increase in the radiation resistance, which is proportional to the number of vertical elements (6 dB of gain improvement by increasing 4 times the number of elements). Further enlargement of the grid produces more intense power dissipation on the conductors and within the surrounding tissues. The optimal efficiency arises for a grid-array of four cells, with a maximum  $\eta = 35\%$  (with corresponding gain  $G_{max} = 6\text{dBi}$ ); then gain slowly improves thanks to the more directive radiation pattern produced by a larger structure.

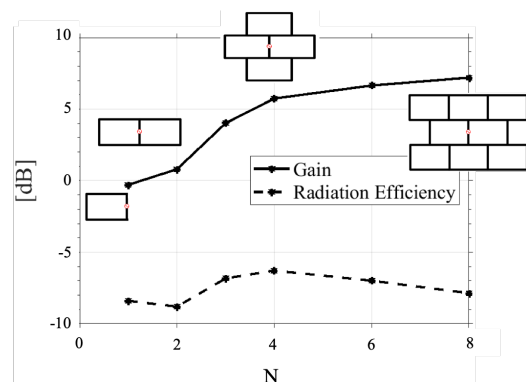


Figure 2. Gain and radiation efficiency of the reference twin-grid by varying the number of elements  $N$ . Efficiency is strongly affected by the radiation losses into the human body, caused by the attenuation of currents on the microstrip lines.

### B. Optimal reflector size

Gain and efficiency of the optimal 4-element twin-grid array are shown in Figure 3 by varying the trace width  $w_r$  of the reflecting grid. As  $w_r$  increases, the breathable area  $BA\% = [(l - w_r) \cdot (s - w_r)] / (l \cdot s)$  decreases with a better decoupling between body and array and consequently an improvement of both gain and efficiency. The size of the reflector affects the radiation performance especially in the early stages. A reduction of  $\sim 15\%$  of the breathable area ( $w_r = 3 \text{ mm}$ ) with respect to the ungrounded structure ( $BA = 100\%$ ) corresponds to an improvement of gain and efficiency of about  $6\text{dB}$  (more than double read distance with respect to the ungrounded structure). By reducing BA up to 50% ( $w_r = 10 \text{ mm}$ ) performance can be further improved, with  $G_{max} \approx 7\text{dBi}$  and  $\eta = -5\text{dB}$ . An asymptotic profile is then observed. Overall, for  $w_r > 10 \text{ mm}$  there is only a modest improvement of the performances at the expenses of bulkiness of the device. Thus, a reasonable choice of the reflector parameter could be  $8 \leq w_r \leq 10 \text{ mm}$ .

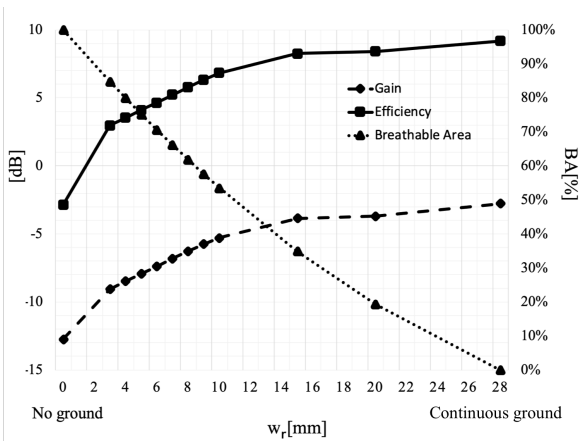


Figure 3. Gain, radiation efficiency and breathable area of the 4-elements twin-grid by varying the width of the reflector trace  $w_r$ .

### III. DESIGN OF A PROTOTYPE AND TESTING

A prototype of the 4-element twin-grid array with  $w_r = 8\text{mm}$  has been fabricated and experimentally characterized. Since backscattering transponders like in UHF band are not available yet<sup>1</sup> at 3.6GHz, the grid has been matched to  $Z_l = 50\Omega$ . The array is now fed through the T-match (Figure 4 a.), useful also for post-production manual tuning to compensate for possible effects of human variability and prototyping uncertainties.

Starting from  $\lambda_{wg}$ ,  $s$  and  $l$  have been slightly varied such to obtain the proper pattern of current (Figure 4 b.) at the operating frequency  $f_0 = 3.6\text{GHz}$ , corresponding to 7 dipoles radiating in phase. The resonant grid alternates series and parallel resonances, as shown in Figure 5 by acting on the length of  $\{a, b\}$  the input impedance  $Z_{in}$  has been modified such to match  $Z_l$  ( $Z_{in} = 53.4 + 0.5 \text{ } \Omega$ ). The final design

<sup>1</sup>For preliminary testing, a diode modulator based on discrete components can be used to emulate the effect of an IC transponder [19].

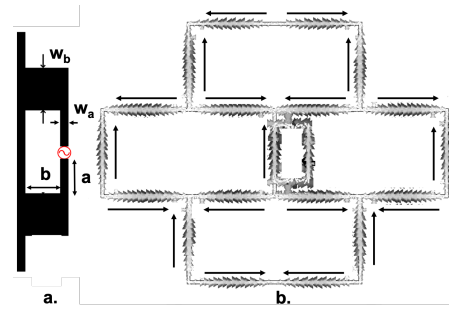


Figure 4. a) Detail of the feeding modality through a T-match transformer to finely control the input impedance of the grid array. b) Pattern of current of the resonant 4-element epidermal grid array with parameter in Table 1 .

parameters are listed in Table I. For other combinations of  $\{a, b\}$  parameters, inductive reactances, as required for matching typical RFID IC impedance, can be synthesized as well [17].

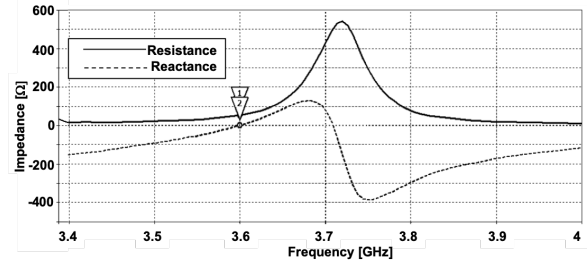


Figure 5. Simulated input impedance  $Z_{in}$  of the 4-cell twin-grid array (parameters in Table I). Parallel and series resonances alternate; by acting on the shape factor of the T-match, the antenna can be matched to  $Z_l = 50\Omega$ .

Radiation pattern is shown in Figure 9. A maximum broad-side gain  $G_{max} = 6\text{dBi}$  ( $BW_{V,-3\text{dB}} = 54.6^\circ$ ,  $BW_{H,-3\text{dB}} = 34.5^\circ$ ) and a radiation efficiency  $\eta = -5.5\text{dB}$  are achieved.

Under simplified hypothesis (free-space interaction, impedance matching, polarization alignment), the maximum reading range can be derived from the Friis Equation [3]. Since 5G-oriented electronics for backscattering radios are not yet available, it will be hereafter assumed that the powers radiated from the reader ( $EIRP = 3.2\text{W}$ ) and the sensitivities of current state-of-the-art UHF-RFID sensing-oriented components ( $P_{chip} = -15 \text{ dBm}$ ) could be achieved for 5G frequencies as well [6]. A maximum read distance of  $d = 4 \text{ m}$  could be hence obtained.

The grid has been fabricated by carving out adhesive copper (thickness  $25\mu\text{m}$ ) by means of a two-axis cutter (Secabo S60). As a benchmark, the full-ground layout has also been fabricated and tested. The final prototype is shown in Figure 6

Table I  
PARAMETERS OF THE REALIZED PROTOTYPES

	$s$	$l$	$h$	$a$	$b$	$w_r$	$w$	$w_a$	$w_b$
Twin-grids	28.45	56.9	2	10	8	8	1	1	4
Full Ground	28.25	56.5	2	8	6.8	28	1	1	5

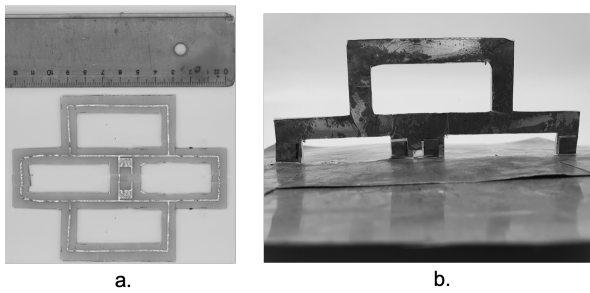


Figure 6. Prototypes of the twin-grids array. a) Front view, b) Back view of the measured half structure.

### A. Measurements

Grid arrays were experimentally characterized by exploiting the image principle. A planar half-structure was vertically mounted on a large ground plane (size  $1m \times 1m$ , more than 10 wavelengths from the radiating elements in each direction) and attached onto a cubic body phantom (roasted pork with estimated parameters  $\epsilon_r = 40$ ,  $\sigma = 2S/m$  [6]) as shown in Figure 7. A  $l_m = 20mm$  wire monopole probe placed at a distance  $r = 13cm$  from the grid array was included to indirectly evaluate the radiation performances of the prototypes. The scattering parameters  $S$  were measured by a VNA (HP 8517A). By assuming that the cables and the network analyzer are perfectly matched, the radiation performances of the epidermal antenna can be retrieved by measuring the  $S_{12}$ , since  $|S_{12}|^2 \propto G$  [16]. For corroboration, the entire system has been numerically evaluated as well.

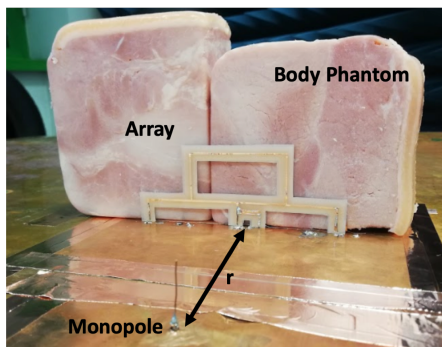


Figure 7. Experimental setup for measuring the  $S$ -parameters of half-grid when attached onto a roasted pork phantom.

Both antennas were slightly manually tuned at  $3.6 GHz$  by acting on the T-match trace  $w_b$  to compensate for uncertainties in realization and phantom. Consequently, a good matching was obtained (Figure 8), in agreement with the simulations. Bandwidth  $BW_{-10dB} = 8.6\%$  is larger than the expected one, probably due to additional losses in the phantom, glue and coaxial cables. The measured  $S_{12}$  of the structure with the grid reflector is approximately 3dB lower than the one of the full ground layout, as visible in Figure 9. By rotating the grid antenna with respect to the monopole probe,  $|S_{12}(\phi)|^2$  has been evaluated also for different angles  $\phi$  on the horizontal plane. Agreement with simulation is maintained. It is worth mentioning that this array configuration is body-matched i.e.

it generates a broadside radiation only when it is placed on the skin. In the free-space, instead the reflector grid is ineffective and a bidirectional pattern is produced.

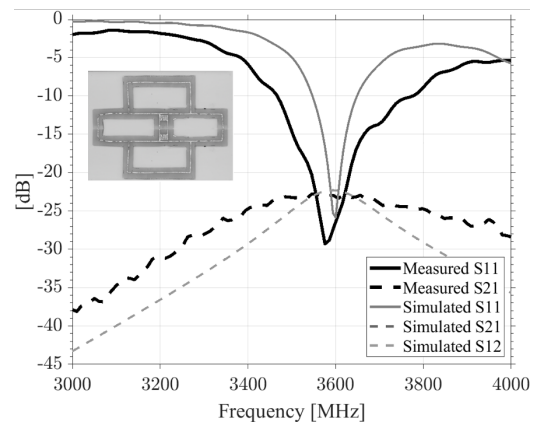


Figure 8. Simulated and Measured S-parameters of the half twin-grid array sourced by a test monopole.

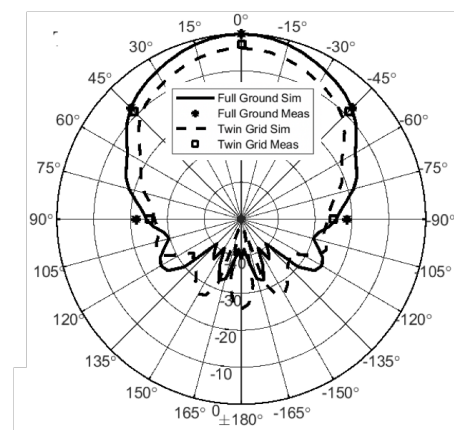


Figure 9. Measured  $|S_{12}|^2$  on the horizontal plane overlapped on simulated data. Data normalized with respect to the full ground maximum

## IV. CONCLUSIONS

A soft and breathable grid array antenna has been simulated and fabricated for on-body epidermal applications at the 5G sub 6-GHz band. The array is suitable to be applied in different body regions such as abdomen, shoulder and back. Promising results have been obtained in terms of impedance matching and gain. With respect to the single loop, a configuration with 4 cells offers a radiation gain 6dB higher, corresponding to a doubling of the expected read distances. By considering valid in S-band the actual UHF RFID features (emitted power and IC sensitivities) read distances greater than 3m are expected, even with thin reflector. Such distances could be suitable to continuously track the vital signs of a user within a room thus greatly extending the current performances of UHF epidermal systems.

## REFERENCES

- [1] K. et al, "Epidermal electronics," *Science*, vol. 333, no. 6044, pp. 838–843, 2011.

- [2] S. Han and et al., "Battery-free, wireless sensors for full-body pressure and temperature mapping," *Science Translational Medicine*, vol. 10, no. 435, 2018.
- [3] D. Dobkin, *The RF in RFID, 4th Ed.* Burlington, MA: Elsevier, 2012.
- [4] S. Amendola, C. Occhiuzzi, and G. Marrocco, "More than wearable: Epidermal antennas for tracking and sensing," *Electromagnetics of Body Area Networks: Antennas, Propagation, and RF Systems*, p. 319, 2016.
- [5] N. F. M. Aun, P. J. Soh, A. A. Al-Hadi, M. F. Jamlos, G. A. E. Vandebosch, and D. Schreurs, "Revolutionizing wearables for 5G: 5G technologies: Recent developments and future perspectives for wearable devices and antennas," *IEEE Microwave Magazine*, vol. 18, pp. 108–124, May 2017.
- [6] F. Amato, C. Occhiuzzi, and G. Marrocco, "Epidermal backscattering antennas in the 5g framework: Performance and perspectives," *IEEE Journal of Radio Frequency Identification*, vol. 4, no. 3, pp. 176–185, 2020.
- [7] H. A. Damis, N. Khalid, R. Mirzavand, H. Chung, and P. Mousavi, "Investigation of epidermal loop antennas for biotelemetry iot applications," *IEEE Access*, vol. 6, pp. 15806–15815, 2018.
- [8] S. Amendola and G. Marrocco, "Optimal performance of epidermal antennas for uhf radio frequency identification and sensing," *IEEE Transactions on Antennas and Propagation*, vol. 65, pp. 473–481, Feb 2017.
- [9] P. S. Hall and Y. Hao, eds., *Antennas And Propagation for Body-Centric Wireless Communications*. Norwood: Artech House Publishers, 1st ed., August 2006.
- [10] A. Pellegrini, A. Brizzi, L. Zhang, K. Ali, Y. Hao, X. Wu, C. C. Constantinou, Y. Nechayev, P. S. Hall, N. Chahat, M. Zhadobov, and R. Sauleau, "Antennas and propagation for body-centric wireless communications at millimeter-wave frequencies: A review [wireless corner]," *IEEE Antennas and Propagation Magazine*, vol. 55, pp. 262–287, Aug 2013.
- [11] G. Gao, B. Hu, S. Wang, and C. Yang, "Wearable circular ring slot antenna with ebg structure for wireless body area network," *IEEE Antennas and Wireless Propagation Letters*, vol. 17, no. 3, pp. 434–437, 2018.
- [12] E. Workman, I. Chang, and S. Noghianian, "Flexible textile antenna array," in *2015 IEEE International Conference on Electro/Information Technology (EIT)*, pp. 569–574, 2015.
- [13] C. Occhiuzzi and G. Marrocco, "Monolithic antenna array for epidermal 5g backscattering communications," in *2020 14th European Conference on Antennas and Propagation (EuCAP)*, pp. 1–3, 2020.
- [14] H. Nakano, T. Kawano, and J. Yamauchi, "Meander-line grid-array antenna," *IEE Proceedings - Microwaves, Antennas and Propagation*, vol. 145, no. 4, pp. 309–312, 1998.
- [15] M. Sun, Y. P. Zhang, Y. X. Guo, K. M. Chua, and L. L. Wai, "Integration of grid array antenna in chip package for highly integrated 60-ghz radios," *IEEE Antennas and Wireless Propagation Letters*, vol. 8, pp. 1364–1366, 2009.
- [16] S. Orfanidis, *Electromagnetic Waves and Antennas*. New Jersey: Rutgers University, August 2010.
- [17] G. Marrocco, "The art of uhf rfid antenna design: impedance-matching and size-reduction techniques," *Antennas and Propagation Magazine, IEEE*, vol. 50, pp. 66–79, feb. 2008.
- [18] B. Zhang and Y. P. Zhang, "Analysis and synthesis of millimeter-wave microstrip grid-array antennas," *IEEE Antennas and Propagation Magazine*, vol. 53, no. 6, pp. 42–55, 2011.
- [19] F. Amato, A. Di Carlofelice, C. Occhiuzzi, P. Tognolatti, and G. Marrocco, "S-band testbed for 5g epidermal rfids," in *URSI GASS 2020, Rome, Italy, 29 August - 5 September 2020*, pp. 1–3, 2020.